8° SUPERCONDUCTING BENDING MAGNET IN A PRIMARY PROTON BEAM*

J. Allinger, G. Danby, B. De Vito, H. Foelsche, S. Hsieh,
J. Jackson, A. Prodell
Brookhaven National Laboratory
Upton, New York

Abstract

A large superconducting bending magnet system is in operation in the new beam from the Brookhaven AGS to the 7-ft. Bubble Chamber. Two dipole modules excited to 37kG with a total magnetic length of 4m bend 30 GeV primary protons by 8°. The system has operated routinely for several months, traversed in 3μs by 6×10^{12} protons with a beam power of 30kJ. The magnet modules have been proven to be very rugged and were found immune to operational beam difficulties which give rise to occasional bursts of radiation heating. The system is designed for on-line operation and computer monitoring of parameters with closed loop He refrigeration. The magnets have demonstrated very little training and have been operated to 44kG with both modules identical to computed field predictions to an accuracy of $\sim 1 \times 10^{-4}$ over the useful aperture. These are the first superconducting magnets used in a primary proton beam, and are of a type which can be used in future accelerators.

1. Introduction

The 8° magnet project has met all its design goals. The combination of a very simple conductor with high conductivity corrugated aluminum sheets results in an economical and mechanically precise coil structure which provides very rapid and efficient heat exchange to helium. A solid iron core was used to avoid a stamping die. The same coil construction technique can be used with a laminated split core. Pulsed models with similar construction have demonstrated excellent behavior, with field properties identical to dc for rise rates of ~ 4kG/sec. Errors due to construction and magnetic pressure are evidenced by the magnitude of quadrupole, octupole, and other error fields, and by the non-identity of sextupole, etc. between modules. These fields show the 8° to be considerably more accurate and predictable than other superconducting magnets built to date. Later designs will produce much higher fields combined with the field quality of the best conventional magnets. The method of construction produces a very economical magnet.

2. Magnet Design

The two magnets employ a rectangular "window-frame" iron core surrounding a rectangular cross-section dipole coil package. The magnet cross section, shown in Figure 1, is 37.8cm high by 43.5cm wide. The iron core, which is closely coupled around the coil, reduces the ampere turns required for magnetic fields below saturation by a factor greater than 2. The magnetic images of the coil in the iron simulate extended dipole sheets, producing very uniform fields below 20kG. Above this field the systematic aberrations due to saturation require an auxiliary correcting coil which is approximately an air core sextupole. The excitation required of this correcting coil commences at ~ 20kG and increases linearly to several percent of the dipole ampere turns at 40kG. The combination of the two separate coils, the dipole and the sextupole, permits the generation of precision fields at all levels as well as providing sextupole tuning when desired.

The dipole coil is wound with 340 turns of a conventional NbTi superconducting composite with a rectangular cross section of ~ 1.4mm by 2.9mm. This contains 361 NbTi filaments, 75 microns in diameter, imbedded in copper, and the whole matrix is twisted one turn per inch. The copper to superconductor ratio is 1.25 to 1. A sheet of anodized high purity aluminum is placed between each of the vertical layers of the dipole and correcting coils. These aluminum sheets are grooved to provide helium coolant channels over 50% of one face of the conductor layer and the anodized surface of the aluminum provides additional interlayer insulation in the coil. The good diffusivity and conductivity of the high purity aluminum provides excellent thermal and dynamic stability.

In order to locate the dipole and sextupole coil turns precisely in the magnet, the stainless steel cold bore block of the magnet was machined with grooves to contain the top and bottom racetrack correcting coils, and the outside of the cold bore block was used as a winding fixture to wind the mid plane correcting coil and the dipole coils. Since the superconductor was relatively uniform in size and the aluminum sheets were rolled to close thickness tolerances, the location of each layer of superconductor in the coils was established during winding. Figure 2 shows the coil winding around the end blocks. Iron plates were assembled around the coil package after winding and torqued to provide precompression of the coil package before assembly in the core blocks. Any residual horizontal motion under magnetic pressure is constrained to coherent motion of the coil layer as a whole and results in very small field errors. Coolant channels were provided at the top and bottom of each coil package and liquid helium supply grooves were machined wherever necessary in the cold bore block. Vent holes were also drilled through the magnet core block and inner iron plates at 3.8cm intervals to provide flow paths for helium gas venting.

Liquid nitrogen precooling channels are welded to the core to provide rapid magnet cooldown through a closed loop LN_2 system. Heating coils are also mounted on the outside surface of the magnet iron to provide rapid warm-up of the system if maintenance is required.

The magnet parameters for the 8° dipole are shown in Table I. Figure 3 shows a completed magnet unit.

TABLE I. MAGNET PARAMETERS (4° MODULE)

Aperture (I.D. warm vacuum pipe)	7.3cm
Magnetic field intensity	40kG
Ampere turns (dipole coil)	408,000
Ampere turns (sextupole coil)	18,000
Current (dipole coil)	1200A
Current (sextupole coil)	300A
Current density (dipole coil conductor)	$3.05 \times 10^4 A/cm^2$
Current density (sextupole coil conductor)	$3.0 \times 10^4 A/cm^2$
Stored energy	150kJ per unit
Inductance (dipole coil)	0.2h per unit

3. Test Performance

The superconducting magnets are immersed in liquid helium at a temperature of 4.5°K. They were designed

*Work performed under the auspices of the U.S. Atomic Energy Commission.

to operate at a field of 40kG. The first module reached 44kG after four training quenches; the second after only two, both at about 40kG. An earlier full-scale cross section model 0.5m long, which was much more poorly constructed, required about ten quenches to attain this level.[1,2] Although this model was designed for 40kG, it has been operated to ~ 50kG at which level there is 57kG in the coil due to excessive saturation, and requires essentially 100% of short sample current.

None of these three magnets has ever quenched after its first operation to a given field, except when subjected to extreme proton radiation heating. This observation is based on much experience with repeated thermal cycles between ambient temperature and liquid helium temperature, charging and discharging the magnets in seconds, and discharging the magnet from 25kG very rapidly into a 0.5 Ω resistor by opening a 500A circuit breaker. No potting is used in these coils which are free to shrink azimuthally with respect to the core, and to move into a final position, or set, under magnetic pressure. After initial testing to its highest field, this type of magnet could be assembled for beam or accelerator applications and no subsequent training would occur.

4. System Description

Since this system was envisioned as a forerunner of more extensive superconducting magnet beam transport lines, considerable attention was given to making it a complete "on-line" pilot plant which would require little direct supervision. A 74W helium refrigerator separated from the magnet by ~ 10m of earth shielding and connected to the magnet dewars by 40m of liquid nitrogen shielded transfer lines provides the necessary cooling. The magnet dewars and refrigerator comprise a closed loop system to which auxiliary equipment has been added for the recovery and storage of the helium gas. The magnet, refrigeration, and recovery systems are instrumented for automatic operation and provisions have been made for computer monitoring.

If required, the two magnets (~ 4082kG total mass) can be heated from 4.5°K in ~ 30 hours and can be cooled down from 300°K to 4.5°K in ~ 16 hours so that the total recycling time in case of a magnet warm-up is quite modest.

These magnets have been in operation whenever needed since late October 1973. Although they have been quenched on four occasions due to problems occurring in other beam transport components, they still operate reliably and with no difficulty. Figure 4 shows the 8° magnet in the proton beam.

5. Radiation Heating

Since this system was designed for use in a primary beam, uncertainty existed as to whether or not the external beam pulse would be sufficiently free of stray particles to limit heating of the superconducting coil. These magnets have operated successfully for long periods of time at beam intensities of ~ 6×10^{12} protons per pulse even under abnormal heating conditions. On occasion, during malfunction of other beam transport components; e.g., a trip-out of the upstream quadrupoles, the magnets absorbed several hundred joules of radiative energy in a period of 3μs for a series of pulses without quenching while small incremental pressure increases were observed in the helium dewars. Moreover, operation has been sustained while one jaw of a collimator located ~ 6m upstream from the magnet was protruding into the beam and intercepting about one-half of the beam. On the other hand, gross malfunctions in steering have quenched the magnet. The capacity of these magnets to absorb large beam losses is very significant since hoped-for future superconducting accelerators depend on a reasonable capacity of the magnets to operate with heating due to beam loss. This is the first experimental evidence anywhere bearing on this fundamental question. It should be noted that this type of construction permits very rapid heat exchange and extreme cooling of the coil. The acceptable maximum exposure in 3μs to the coil itself will have to await more controlled experimentation.

6. Magnetic Measurement Results

The two magnet modules were measured separately, prior to final assembly with their warm bore beam tubes which define the maximum aperture of $r_m = 3.653$cm, using a harmonic coil device. These radial field measurements were made at $\rho_c = 3.825$cm which is 76% of the 5cm radius to the superconductors. Each magnet was repetitively cycled to 38kG. Long integrating and internal point measurements were made on both rising and falling sides of the cycle. The radial field is expressed as

$$B = B_o \sum_n \left[a_n \frac{r^n}{\rho_c^n} \cos (n+1)\,\theta + b_n \frac{r^n}{\rho_c^n} \sin (n+1)\,\theta \right] \quad (1)$$

carried out to n = 11. The reference angle, θ = 0, is set at the magnet horizontal midplane. Considerable data were accrued in intensive periods which were restricted to a few days on each magnet by the construction schedule. Simultaneous measurements on the magnets in series are planned when they are not in use for the physics program. The identity of the units can then be more easily and accurately checked, especially for the sextupole component which can be affected by slight differences in excitation currents. Nevertheless, quite accurate conclusions can already be drawn.

Analysis focuses on three parts:

1. With equal excitation currents in each magnet, as if in series, the agreement of the sextupole terms b_2 with each other and with computer predictions.

2. With the auxiliary coil tuned to cancel the sextupole (b_2) in each magnet, the identity of the field aberrations with computer predictions and with each other.

3. The magnitude of terms not allowed by symmetry due to construction and measurement errors. The most critical effect is on the quadrupole terms (2θ), followed by sextupole, etc.

The identity and mechanical precision of the two units are, in fact, very good and appear to be comparable to high quality conventional magnets. The absolute field uniformity, while reasonable when compared with other superconducting magnets constructed to date and being more than adequate for its purpose, is not as good as high quality conventional magnets. These modules were the first magnets of their type designed. It is now known how to make the field below 20kG arbitrarily uniform by design, and how to correct for saturation at high fields with much less aberration resulting.[3] It is believed that a second generation of such magnets should be of conventional magnet field quality from both a conceptual and practical construction point of view.

Table II shows calculated and measured field multipolarities at 24kG for module 1 on a rising field cycle. Column 1 lists the computed multipoles for the "perfectly constructed" magnet. Column 2 gives the corresponding measured internal fields. Column 3 gives the long coil results. Column 4 is the difference

(i.e., Columns 3-2) or the contribution due to the ends. Column 5 lists results of a separate experiment wherein the short coil and the long coil were hooked in series opposition to measure end effects directly. This should be more accurate than Column 4. The agreement gives some measure of precision.

TABLE II. 8^{o} MAGNET (#1) B_o = 24kG

$\frac{(n+1)\theta}{1\theta}$	1 Computer		2 Measured Point Coil		3 Measured Long Coil		4 (3-2)		5 Measured Long-Point	
	a_n	b_n	a_n	b_n	a_n	b_n	a_n	b_n	a_n	b_n
$3\theta/1\theta$	0	+12.2	1.1	+ 2.5	0.3	+1.3	1.4	-1.2	2.3	-3.4
$5\theta/1\theta$	0	+ 9.2	0.1	+11.4	0	+6.8	0.1	-4.6	0.7	-4.6
$7\theta/1\theta$	0	- 6.2	0.1	- 7.4	0.1	-4.8	0	+2.6	1.0	+2.5
$9\theta/1\theta$	0	- 3.4	0.1	- 5.2	0	-4.4	0.1	+0.8	1.0	+0.9
$11\theta/1\theta$	0	+ 1.0	0	- 0.1	0.1	+0.2	0.1	+0.3	0.2	0
$2\theta/1\theta$	0	0	1.7	+ 3.3	2.8	+3.4	1.1	+0.1	0.7	+0.2
$4\theta/1\theta$	0	0	0.9	- 0.8	1.4	-0.4	0.5	+0.4	0	+0.2
$6\theta/1\theta$	0	0	1.3	+ 0.2	0.9	+0.1	0.4	-0.1	0.4	0
$8\theta/1\theta$	0	0	0.8	+ 0.3	0.6	+0.2	0.2	-0.1	0.2	-0.3
$10\theta/1\theta$	0	0	0.3	- 0.1	0.2	-0.1	0.1	0	0.1	-0.1

Note: Field multipolarities expressed relative to the dipole field (1θ) in terms of 10^{-4} parts at the measurement radius (ρ = 3.825cm).

The amplitudes in Columns 2 and 3, which are zero in 1, are a measure of magnet construction errors, complicated by measurement errors. Comparison of the many runs, both on the up and down cycle, long and short coil, gives a quadrupole b_2 error of $\sim 3 \times 10^{-4}$ at $r = \rho_c$ (0.8×10^{-4} cm^{-1}). [1]This is present at all field levels. The skew quadrupole term, a_1, is $\sim 1.5 \times 10^{-4}$ (0.4×10^{-4} cm^{-1}). The quadrupole error happens to be roughly equal in both magnet modules. The higher order terms not allowed by symmetry, when data from all the $\sim$ 50 runs both up and down are examined, show no systematic presence and are consistent with being measurement errors. At the measurement radius the quadrupole is about three times larger than the estimated measurement error. This is consistent with higher order errors due to mechanical asymmetry being equal or smaller than measurement accuracy. The difference between predictions and measurement for terms allowed by symmetry will be discussed later. Briefly, in Columns 1 and 2, the (3θ) b_2 offset is due to iron hysteresis common to both magnets. It is small, well behaved with field, and is well known in conventional magnets. Computations ignore hysteresis which can be corrected by a slight change of the auxiliary coil current.

Table III lists, for both units at three fields on a rising cycle, the internal multipoles b_n allowed by symmetry, plus their out-of-phase equivalent a_n, as a rough indicator of accuracy. For these, and all the runs, the difference between the two units is small and well predicted by computations. (The 38kG b_2 difference shown in Table III happens to be the largest discrepancy found.)

There exists a small design field difference between the two magnets. After the winding of a dipole coil vertical layer, a few thin shims are located between conductors in known positions so that the layer is tight in predetermined locations between its boundaries. The size of the initial length of the Formvar coated rectangular conductor used for the inner layers of the first magnet varied along its length. Thereafter the size settled down to a constant tolerance. When the second magnet was started, it required different shims consistent with the outer layers of number 1. The correct shim locations were computed rapidly when the problem arose, using block approximations to the coil, and gave an arrangement with essentially identical field multipoles. Later, more accurate calculations using actual location of the conductor layers revealed a small difference between the magnets. In retrospect, this problem presented a method for fine tuning. A few predetermined calculations permit the location of spacings to be used in both the design and construction to flatten the low field properties to great accuracy. It should be noted that following a lead burnout and resulting coil arc, number 1 module had the outer layers of the coil removed. The coil was spliced and rewound

TABLE III. COMPARISON OF UNITS 1 AND 2

$\frac{(n+1)\theta}{1\theta}$	Magnet Unit	6kG		24kG		38kG	
		a_n	b_n	a_n	b_n	a_n	b_n
$3\theta/1\theta$	1	2.7	+ 4.0	1.1	+ 2.5	0	- 6.4
	2	0.1	+ 4.3	0.3	+ 1.7	0.1	- 1.9
$5\theta/1\theta$	1	0.1	+17.6	0.1	+11.4	0.4	-15.6
	2	0.4	+18.0	0.3	+12.5	0.1	-14.1
$7\theta/1\theta$	1	0.1	-10.1	0.1	- 7.4	1.4	- 2.0
	2	0.2	-11.0	0.2	- 8.5	0.9	- 2.1
$9\theta/1\theta$	1	0.5	- 1.8	0.1	- 5.2	0.1	-32.6
	2	0.2	- 1.6	0.2	- 4.9	0	-32.5
$11\theta/1\theta$	1	0.1	- 1.0	0	- 0.1	0.5	+ 3.9
	2	0.2	- 1.2	0	+ 0.1	0.4	+ 2.9

Note: Field multipolarities expressed relative to the dipole field (1θ) in terms of 10^{-4} parts at the measurement radius (ρ = 3.825cm).

without difficulty. It was after the repair that the magnet module was measured and put to use.

We return to the question of the precision and identity of the two units. The largest error is the quadrupole, $G/B_o \sim 0.8 \times 10^{-4}$ cm^{-1} for each magnet. The next largest effect expected is on the identity of the sextupoles. Figure 5 shows point coil sextupole data for identical current excitations of both magnets. The baseline corresponds to average $b_2 = 0$ for the computed magnets. Because of the computational errors during construction described earlier, these excitations more accurately produce the computed b_2 values shown in curves (L_1) and (L_2). For rising fields, experimental b_2 are plotted and their average, curve (M). Also plotted is the corresponding falling field data and curve (N). The offset of curve (M) from the baseline is due to hysteresis on a rising cycle. The offset between curves (M) and (N) is the width of the single sided hysteresis loop. Note that the downside is further than the upside from the computed baseline, as it should be, since the computed magnets have no hysteresis. For comparing the two magnets the down-cycle is as valid as the up cycle. The difference between magnets as measured and computed is in agreement to a very small error consistent with measurement accuracy for the great bulk of the data. It is evident that the module 2 point at 18kG on curve (M) is in error. The other points at 18kG on curves (M) and (N) are normal. An identical graph for long coil results (not shown) has no irregularity at 18kG and constant loop width between the up and down cycles. The 38kG data shows some deviation beyond expected measurement accuracy, as also seen in b_2, Table III. The long coil data suggests that if this magnet difference is real, it is considerably smaller than indicated in Figure 5. Separate run data taken at 40kG does not show this deviation. Further experimentation will have to clarify if there is a very small high field difference. Since these magnets have solid iron rather than mixed and stacked laminations, some small permeability effects are possible. Finally, if the 1-2 differences for all runs are averaged and compared with the equivalent computed differences, agreement is good to a number small compared to 1×10^{-4}. The evidence strongly suggests that real sextupole magnet errors are less than measurement errors and are $\leq 1 \times 10^{-4}$ (0.06×10^{-4} cm^{-2}) to go along with the quadrupole error of $\sim 3 \times 10^{-4}$ (0.8×10^{-4} cm^{-1}). This is respectably small even for conventional magnets.

Consider next the higher multipoles from the viewpoint of predictability and of absolute field quality. The 5θ, point coil, field measurements show very small hysteretic effects ($\sim 1 \times 10^{-4}$). The up and down cycles are mutually displaced as in Figure 5, but only by about 0.5×10^{-4}. The absolute agreement of computer and experiment for both magnets is very good with a constant offset of 3×10^{-4}. This includes any small hysteresis, plus systematic permeability or computer fitting effects, etc. The amplitude of 5θ varies considerably with field level, and this is followed exactly by the computations. The fact that the computer predicts the shape of 5θ very accurately is important, since the 8° magnets have a large built-in 5θ, considerably larger than in the later designed 20-in. long model.

The 5θ term has the only significant superconducting diamagnetism in this magnet design. Internally, $b_4 \sim 6 \times 10^{-4}$ is produced on the up-cycle at 6kG, and is very small by 12kG. This diamagnetism is due to the correcting coil used.[4] Diamagnetism in the dipole coil returns primarily through the iron to high approximation.

For 7θ, 9θ, and 11θ no hysteretic or diamagnetic effects are evident, and the magnet differences are predicted to better than 1×10^{-4}. Again, as the amplitude changes with field, the predictions of absolute value follow the shape closely. Systematic offsets at the level of a few parts in 10^4 occur, as in 5θ.

With sextupole tuned to zero, the magnetic field uniformity of each magnet at 6kG is shown in Figure 6B. The horizontal midplane field (H1) of magnet 1 and (H2) of magnet 2 was reconstructed at several radii and this data plotted. Points (V1) and(V2) are the equivalent vertical midplane data. The computer predictions are shown by the two solid curves. For clarity of presentation, the computed fields of magnets 1 and 2 were averaged. Thus HCOMP is the average computed horizontal midplane, and VCOMP is the vertical equivalent. For perfect predictability and measurement, HCOMP should pass through the average of H1 and H2. Quadrupole field is not included and must be treated as a superposition. The absolute field nonuniformity is $\leq 10 \times 10^{-4}$ at the beam tube on both midplanes and at all angles θ. At the measurement radius ρ_c, computer and experimental average deviate by $\sim 1.5 \times 10^{-4}$. It is important to note that the model, which was of a somewhat later conceptual design, was uniform to $\sim 1 \times 10^{-4}$ up to the beam tube; i.e., ~ ten times more uniform than the 8°.

While absolute field quality is reasonably good, Figure 6A shows the predictability is of a much higher order. This contains the same information, but now only the differences between the two magnets are plotted. Note the scale change. The differences are very small and predicted to $< 1 \times 10^{-4}$.

Figure 7 gives the same information at 30kG. The field nonuniformity is now somewhat larger and the deviation from prediction is larger. The vertical computer curve, VCOMP, lies quite close to the experimental points. The HCOMP curve is off even at r = 60%. This is due to the systematic offsets between experimental and computed multipoles described earlier. However, the magnet difference data in Figure 7A is again predicted to $< 1 \times 10^{-4}$.

Figure 8 gives the same results at 38kG. The useful field radius is shrinking, due mainly to the large 9θ produced by the correction coil design. Again VCOMP agrees quite well with both magnets, but HCOMP by $r = \rho_c$ differs considerably. However, in Figure 8A the differences between magnets are predicted very accurately with an error $< 1 \times 10^{-4}$. It should be noted that, as was the case at low fields, the field uniformity of the model was much better than the 8°. The field uniformity $\Delta B/B_o$ was within 1×10^{-4} to 62% of aperture at 38kG. Nevertheless, the differences between the measured and the predicted model were about equal to those in the 8° case, showing the same systematic effects due to hysteresis, computer program, etc.

In summary, except for small hysteretic and other effects common to both, the 8° magnets have shown allowed multipoles which are predictable to high accuracy. The predicted small difference between the two magnets due to construction problems which are now under control comes very close to the difference between the two magnets as measured separately. This means that the construction and measurement errors are very small, and the ability to iterate, in the future, small absolute deviations between computations and reality is ensured. This was the first design of this type. The full cross section model was a considerable improvement, and later designs provide very uniform fields at all levels. With the same precision of construction as in the 8°, field quality equivalent to the best of conventional magnets seems feasible.

Finally, a brief comment on end effects. No attempt was made to design the ends for field shaping.

Nevertheless, the b_2 contribution of ends to the field integral remains within $\sim 10 \times 10^{-4}$ parts over all excitations. This, like the iron hysteresis of similar magnitude, can simply be absorbed into the defined auxiliary coil current required for all magnets so that the b_2 integral is made zero at all fields. The 5θ contribution is roughly constant, at -4×10^{-4}. To the extent this is constant, it can be handled simply by a compensating internal offset in computed design. The low field 5θ end effects due to diamagnetism in the superconductor happen to cancel the internal contribution of 6×10^{-4} at 6kG, so that the 5θ integral on the rising field is equal at 6kG and 12kG. The 7θ term measures $+2.5 \times 10^{-4}$ and is very constant over the entire field range, so it can be taken care of by internal design. The 9θ and 11θ have negligible end effects. Without any attempt at end shaping, end effects should be smaller than in typical conventional magnets used in beams and accelerators.

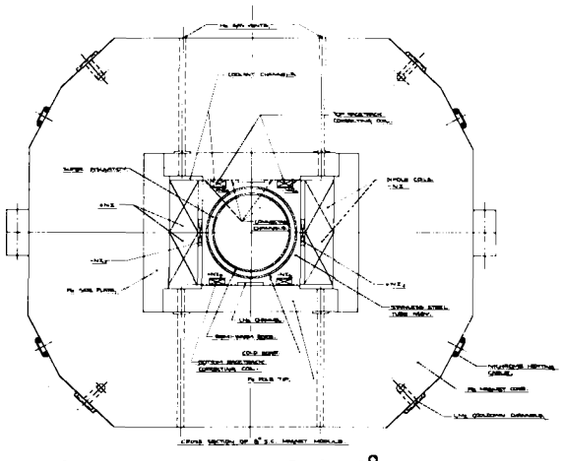

Fig. 1. Cross section of the 8° superconducting magnet.

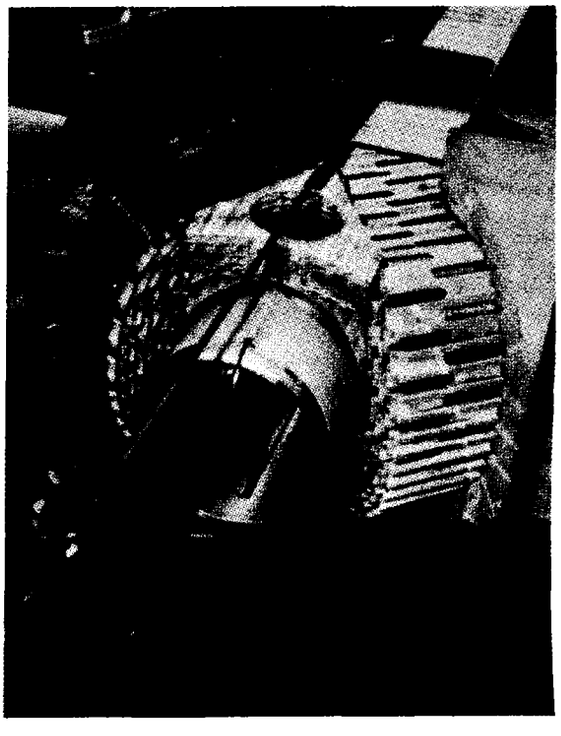

Fig. 2. Superconductor being wound around magnet end blocks.

References

1. J. Allinger, et al., IEEE Trans. Nucl. Sci. NS-20, No. 3 (1973).
2. J. Allinger, et al., in Proc. of the Fourth Intl. Conf. on Magnet Technology (CONF-720908) p. 637 (1972).
3. J. Allinger, et al., Proc. of this Conference.
4. G. Danby, et al., in Proc. of the Fourth Intl. Conf. on Magnet Technology (CONF-720908) p. 334 (1972).

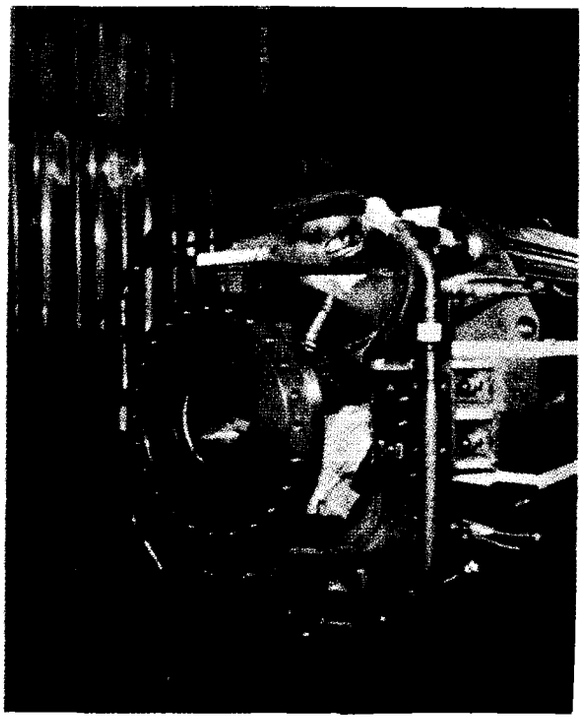

Fig. 3. End view of 8° superconducting magnet module.

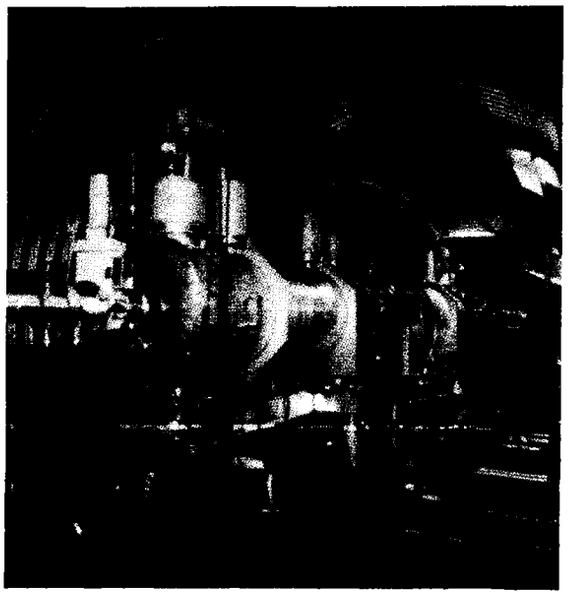

Fig. 4. 8° magnet system installed in North Area tunnel.

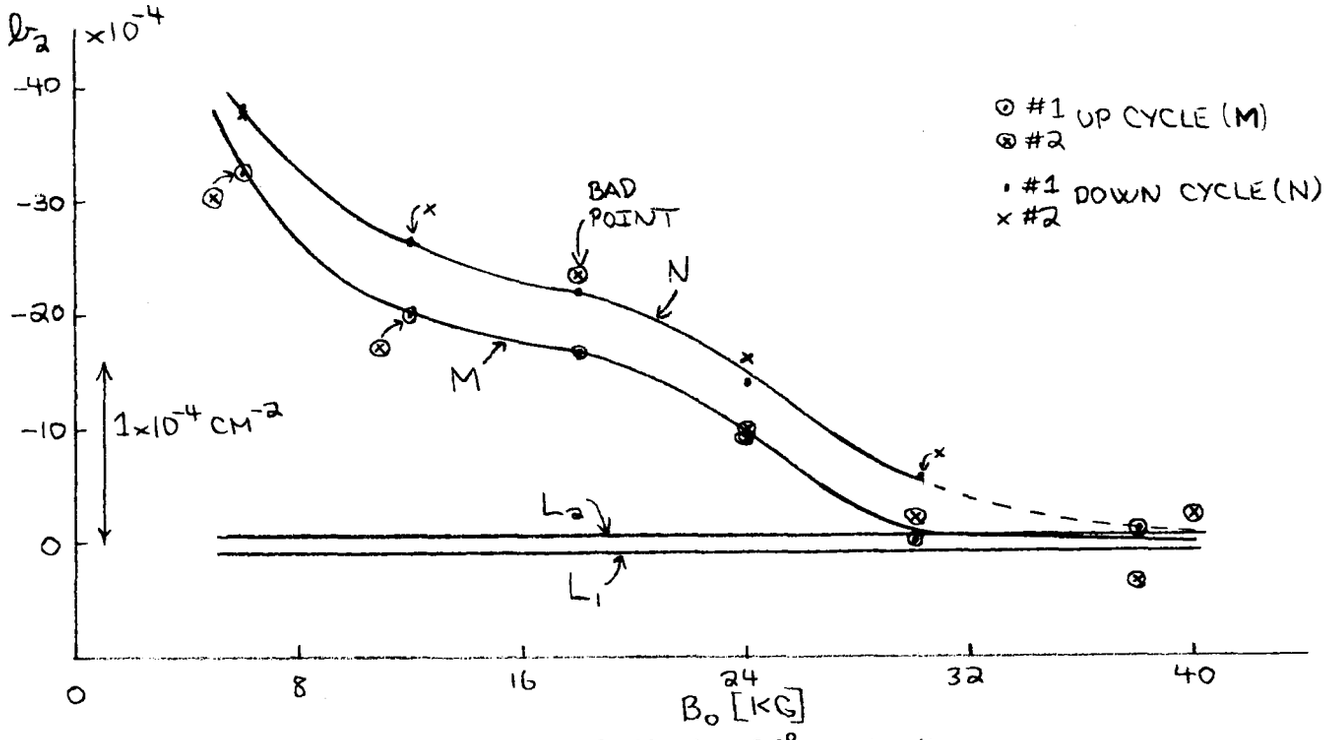

Fig. 5. Sextupole identity of 8° magnet units.

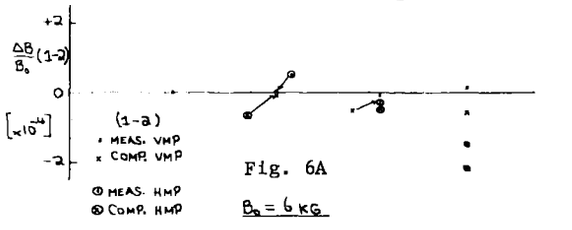

Fig. 6A

$B_0 = 6$ KG

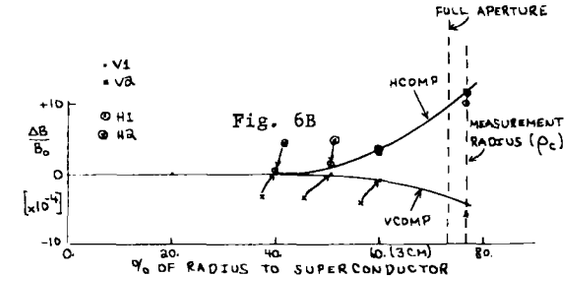

Fig. 6B

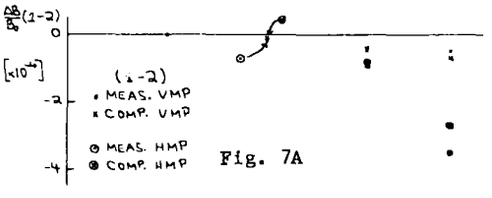

Fig. 7A

$B_0 = 30$ KG

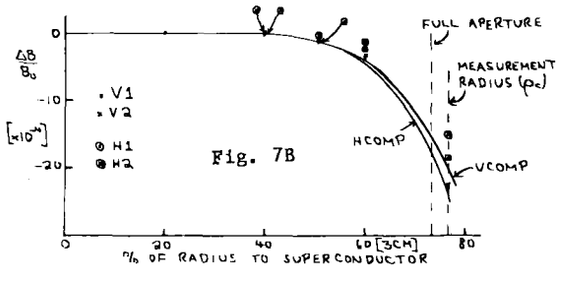

Fig. 7B

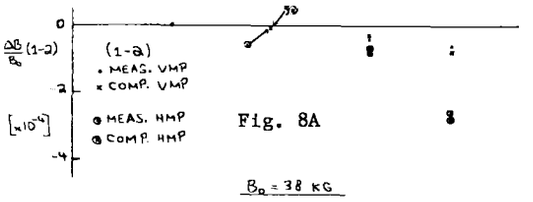

Fig. 8A

$B_0 = 38$ KG

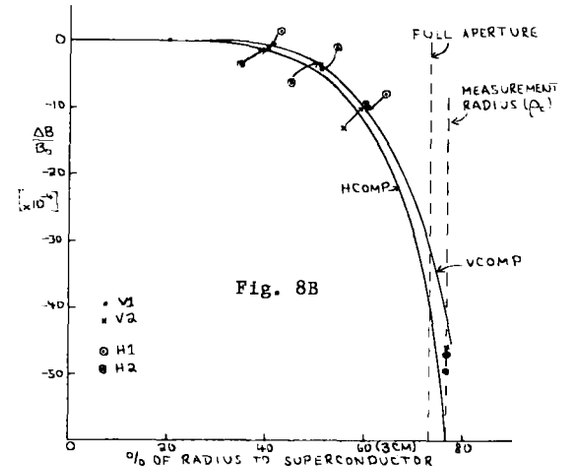

Fig. 8B